

# Characterization of a New Silicon Photomultiplier in Comparison with a Conventional Photomultiplier Tube

Behnoush Sanaei<sup>1</sup>, Mohammad T. Baei<sup>2\*</sup>, S. Zahra Sayyed-Alangi<sup>2</sup>

<sup>1</sup>Faculty of Engineering, University of Wollongong, Northfields Ave, Wollongong, Australia

<sup>2</sup>Department of Chemistry, Azadshahr Branch, Islamic Azad University, Azadshahr, Iran

Email: \*[Baei52@yahoo.com](mailto:Baei52@yahoo.com)

Received 4 March 2015; accepted 19 March 2015; published 25 March 2015

Copyright © 2015 by authors and Scientific Research Publishing Inc.

This work is licensed under the Creative Commons Attribution International License (CC BY).

<http://creativecommons.org/licenses/by/4.0/>



Open Access

---

## Abstract

A Silicon Photomultiplier (SiPM) array (ArraySM-4p9) from the SensL Inc. has been evaluated in this study. The current-voltage (I-V) characteristics of individual SiPM pixels were measured. Then the energy spectral performances of this SiPM array were evaluated with different scintillator samples as compared with a conventional PMT of Hamamatsu 878. The used scintillator samples include GAGG: Ce ( $3 \times 3 \times 6 \text{ mm}^3$ ), CsI (TI) ( $3 \times 3 \times 6 \text{ mm}^3$ ), and LYSO ( $2 \times 2 \times 5 \text{ mm}^3$ ). The energy spectra of these scintillator samples with a SiPM pixel were measured using gamma-ray sources of  $^{57}\text{Co}$  (122 keV),  $^{22}\text{Na}$  (511 keV) and  $^{137}\text{Cs}$  (662 keV) and were compared with the conventional PMT. The measured I-V curves of this SiPM device have shown good performance uniformity over the  $4 \times 4$  SiPM array units. The channel-to-channel variations of the 16 SiPM pixels in the breakdown voltages, gains and dark currents are very consistent and stable. Gamma spectroscopy using  $^{57}\text{Co}$ ,  $^{22}\text{Na}$  and  $^{137}\text{Cs}$  sources shows that this SiPM device has well comparable spectral performance as the conventional PMT. The SiPM with CsI (TI) and GAGG: Ce crystals using  $^{57}\text{Co}$  source show significant better energy resolutions than the conventional photomultiplier tube (PMT) for the low energy gamma-ray detections. Finally, the newly available SiPMs show very good properties and are well suited with most common used scintillation crystals for gamma-ray detections in a broad energy range. The SiPM has a great promise to replace the conventional PMT.

## Keywords

Conventional Photomultiplier Tube (PMT), Silicon Photomultiplier (SiPM), Gamma-Ray, Spectroscopy, Energy Resolution

---

\*Corresponding author.

## 1. Introduction

The photomultiplier tube (PMT) has been serving us as a primary photo-detector for over 70 years [1] [2]. PMTs are the extremely sensitive detectors of light in the ultraviolet, visible, and near-infrared ranges of the electromagnetic spectrum that consist of an input window, a photocathode, focusing electrodes, an electron multiplier and an anode usually sealed into a evacuated glass tube [3] [4]. It is based on the vacuum-tube technology resulting in some major limitations, such as bulky size, low quantum efficiency (25%), relatively high cost and sensitiveness to the magnetic fields. Great efforts have been put into investigating and improving solid state silicon devices in order to replace the PMT throughout the past two decades [5]-[8]. Recently, the Silicon Photomultiplier (SiPM) has been emerged as a promising photo-detector technology [9]-[12]. A SiPM typically is composed of a 2-D array of small APDs (called cells or microcells) designed to operate in Geiger-mode. The Silicon Photomultiplier (SiPM) is a novel photon sensing device, with potential applications in particle physics, medical application and general gamma-ray spectroscopy. The high gain, high photo detection efficiency, compact geometry and magnetic field insensitivity of SiPM have shown a great promise to replace the conventional photomultiplier tube (PMT).

According to the comparative studies of new devices of SiPMs and traditional vacuum PMTs by Feng *et al.* in 2011, excellent performance of the SiPMs, such as superb single photon resolution, high gain ( $\sim 106$ ) and low power consumption ( $< 0.1$  mW), is comparable to the conventional PMTs. However, this new kind of technology indicates some drawbacks including very high dark rates ( $\sim 1.9$  MHz/mm<sup>2</sup>) and intrinsic optical crosstalk rates ( $\sim 0.21$  MHz/mm<sup>2</sup>) [12].

The aim of this study is to characterize a new silicon photomultiplier (ArraySM-4p9) from the SensL Inc. and the gamma radiation spectroscopy that incorporates this SiPM coupled to a scintillation crystal in order to compare the results in comparison with PMT gamma spectroscopy.

## 2. Methodology

The property of the SiPM is characterized by the current-voltage (I-V) curve. A SiPM from SensL Company called ArraySM-4p9 was investigated. As it can be seen from **Figure 1**, this SiPM composed of nine array packages arranged in the  $3 \times 3$  format so that, every array has sixteen pixel elements (overall, 144 pixels). Each of the array packages has its own +HV bias connection, and each pixel has its own current connection. To obtain the I-V curve, the currents for different values of bias voltage are measured for individual SiPM pixels. Since the breakdown voltage of this detector is 27.6 volts, the range of bias voltage was chosen between 20 V to 34 V. This measurement was done to determine whether all the pixels show the uniform I-V curve or not.

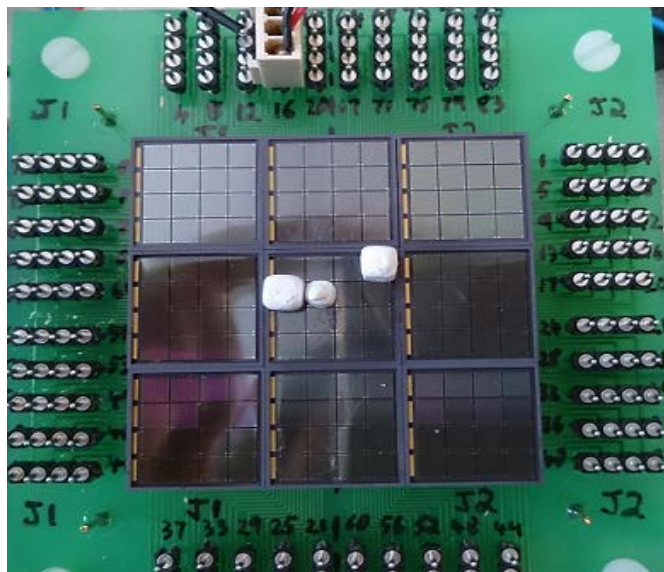


**Figure 1.** Scintillation crystals (LYSO, GAGG and CsI) placed on different pixels of SiPM.

To measure the gamma ray spectroscopy with Silicon photomultiplier, the gamma sources with different energy were mounted upon the scintillation crystal of different size and different material placed on an ArraySM-4p9 SiPM (see **Figure 2**).

These gamma rays used were  $^{137}\text{Cs}$  (high energy),  $^{22}\text{Na}$  (medium energy) and  $^{57}\text{Co}$  (small energy) and the scintillation crystal included LYSO ( $2 \times 2 \times 5 \text{ mm}^3$ ), GAGG ( $3 \times 3 \times 6 \text{ mm}^3$ ) and CsI ( $3 \times 3 \times 6 \text{ mm}^3$ ). So that, LYSO, GAGG and CsI were placed on different microcells of SiPM, numbers 67, 68 and 69, respectively. Then the voltage and current cable were connected to corresponding pin of Array SiPM to obtain gamma spectrum (**Figure 2**).

The software used in this experiment is called Amptek. This program provide the gamma spectrum including some information such as, Centroid and FWHM that are number of channels at the centre of photo peak and Full Width at Half Maximum, respectively. Using this information, the energy resolution can be obtained from the following equation:

$$\text{Energy resolution} = \text{FWHM}/\text{Centroid} \quad (1)$$

To measure the gamma ray spectroscopy with PMT, the gamma sources with different energy were mounted upon the scintillation crystal of different size coupled to a photomultiplier tube (**Figure 3**).

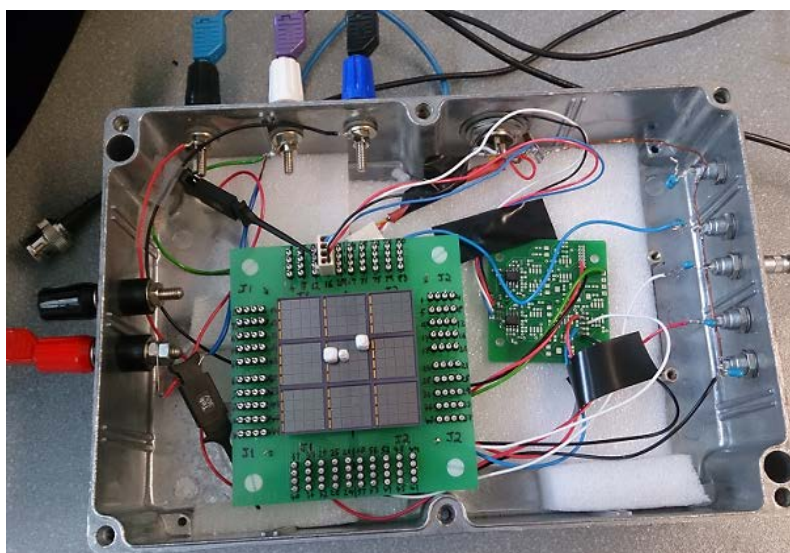


**Figure 2.** Spectroscopy set-up.



**Figure 3.** (a) Scintillation crystal coupled to Hamamatsu photomultiplier tube (R878); (b) Gamma source mounted upon the crystal.

Then the PMT was connected to voltage supply (1300 volts), preamplifier, amplifier, multichannel analyser and computer respectively, to show the gamma spectrum (see **Figure 4**).

These gamma rays include  $^{137}\text{Cs}$  (high energy),  $^{22}\text{Na}$  (medium energy) and  $^{57}\text{Co}$  (small energy) and the scintillation crystal used were NaI (big size), LYSO ( $2 \times 2 \times 5 \text{ mm}^3$ ), GAGG ( $3 \times 3 \times 6 \text{ mm}^3$ ) and CsI ( $3 \times 3 \times 6 \text{ mm}^3$ ). The software used in this experiment is same as used for SiPM, Amptek providing the gamma spectrum from PMT. The information from the spectrum includes Centroid and FWHM used to calculate energy by Equation (1).

### 3. Results and Discussion

#### 3.1. Characterization of the I-V Curve of This SiPM Detector

The curve plotted for this experiment (**Figure 5**) shows current versus bias voltage for a number of ArraySM-4p9 pixels (from pixel 0 to pixel 16).

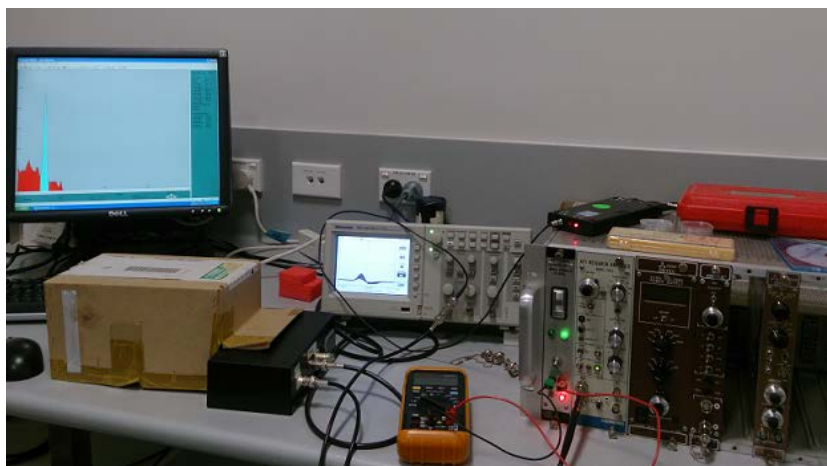


Figure 4. Spectroscopy set-up.

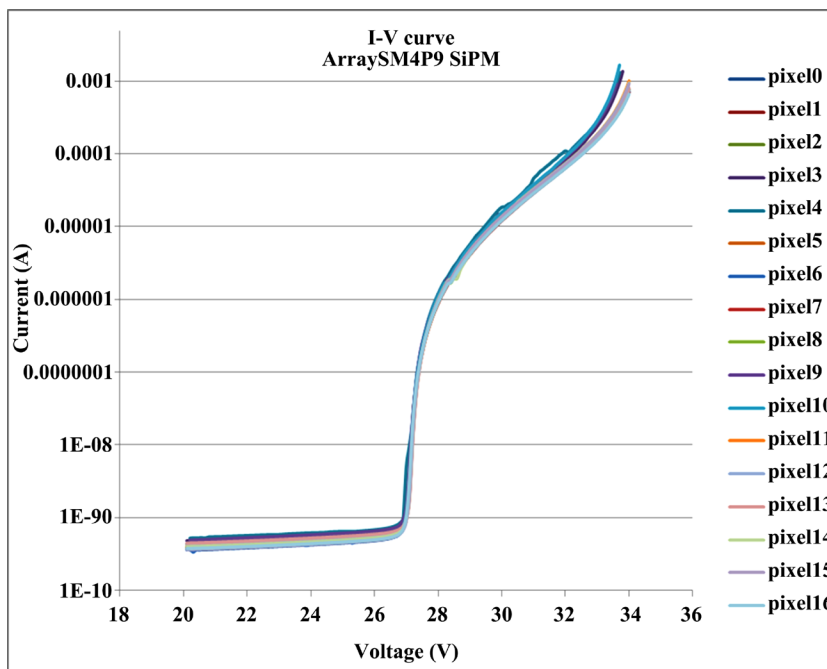


Figure 5. Current vs. voltage for different pixels of ArraySM-4p9 SiPM.

The study of SiPM in the absence of light provides valuable information on its characteristics. The current-voltage I-V curve obtained by measuring the current for different values of the reverse bias voltage allows determining essential information of functionality of the SiPM. **Figure 5** shows the I-V curve from ArraySM-4p9 SiPM. As it can be seen from this figure, in the first part of the curve, for bias voltage below the breakdown voltage (27.6 volts), the current measured is the surface leakage current, which increases with the bias voltage but not significantly. Above the breakdown voltage, the current is the sum of the leakage and the breakdown currents. The breakdown current increases with the gain and dark rate which both depend linearly on the bias voltage. From the I-V curve, the important operating parameters of SiPM, such as breakdown voltage, dark current and gain, can be extracted. From **Figure 5**, all the 16 SiPM pixels show very consistent behaviour. The channel-to-channel variations in breakdown voltages and dark currents are very small. These indicate that this SiPM array module has very good performance uniformity and stability

### 3.2. Spectroscopy Characteristics of the SiPM with Different Scintillation Crystals and Different Gamma Sources

Data taken in this experiment has been calculated using Equation (1). Then the count energy curve has been plotted for fixed gamma source with different crystals (**Figure 6**), and a separate curve for fixed crystal with different gamma sources (**Figure 7**). Furthermore, **Table 1** compares the data taken from gamma ray spectrum of different gamma sources and different scintillation crystals using SiPM. Gamma spectroscopy is used to determine the identity and quantity of gamma-emitters in gamma sources. The spectrum obtained from Silicon Photomultiplier coupled to scintillation crystal using gamma source determines essential information of functionality of the SiPM.

In this research, the gamma spectrometer using SiPM is developed. **Figure 6** illustrates the  $^{137}\text{Cs}$  spectrum from ArraySM-4p9 SiPM coupled to different scintillation crystals including CsI (4.51 g/cm<sup>3</sup> density: 3 × 3 × 6 mm<sup>3</sup>), LYSO (7.1 g/cm<sup>3</sup> density: 2 × 2 × 5 mm<sup>3</sup>) and GAGG (high density: 3 × 3 × 6 mm<sup>3</sup>). From **Figure 6** and **Table 1**, it can be concluded that CsI crystal with lower density provides higher energy resolution in comparison with LYSO and GAGG.

In addition, **Figure 7** compares the spectrum of three gamma sources with different energy acquired with the same SiPM coupled to LYSO scintillation crystal. This comparison indicates the lower energy resolution for higher energy gamma source. So, low energy  $^{57}\text{Co}$  spectrum using LYSO crystal gives a high energy resolution of 21.86% of FWHM. In contrast, high-energy  $^{137}\text{Cs}$  spectrum using the same crystal gives a low energy resolution of 9.25% of FWHM (better energy resolution).

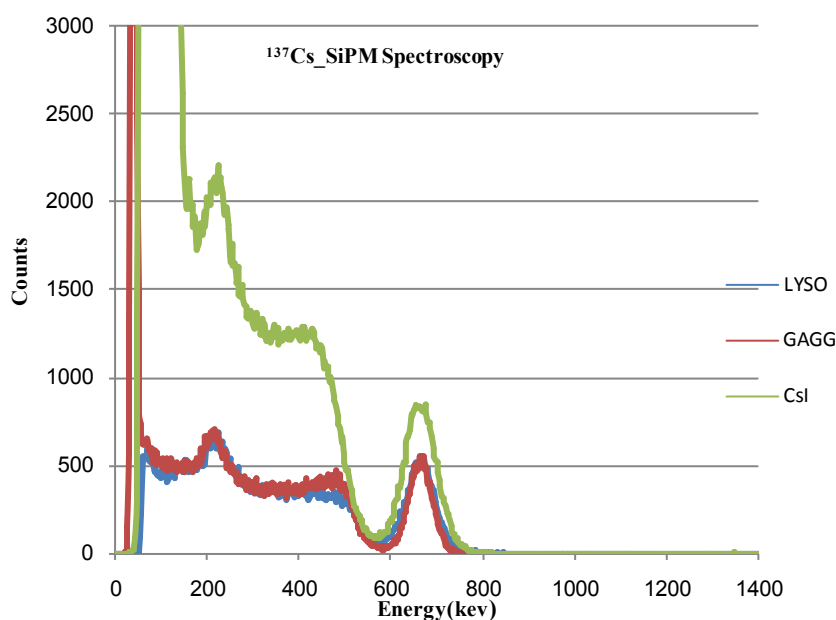


**Figure 6.**  $^{137}\text{Cs}$  spectrum acquired with SiPM coupled to LYSO, GAGG and CsI crystal.

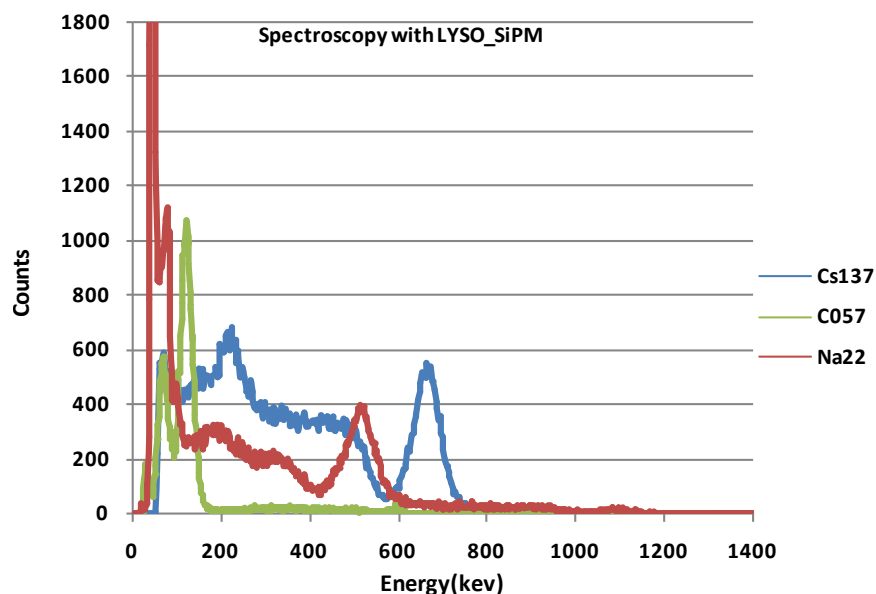


Figure 7.  $^{22}\text{Na}$ ,  $^{57}\text{Co}$  and  $^{137}\text{Cs}$  spectrum acquired with SiPM coupled to LYSO crystal.

Table 1. Data taken from gamma ray spectrum of different gamma sources coupled to different scintillation crystals using SiPM.

SiPM	$^{137}\text{CS}$ (662 keV)			$^{22}\text{Na}$ (511 keV)			$^{57}\text{CO}$ (122 keV)		
	Centroid	FWHM	Energy resolution %FWHM	Centroid	FWHM	Energy resolution %FWHM	Centroid	FWHM	Energy resolution %FWHM
<b>CSI</b> $3 \times 3 \times 6 \text{ mm}^3$	238.89	27.709	11.60%	84.73	12.242	14.45%	77.29	17.044	22.05%
<b>LYSO</b> $2 \times 2 \times 5 \text{ mm}^3$	229.56	21.228	9.25%	251.31	31.935	12.71%	95.00	20.766	21.86%
<b>GAGG</b> $3 \times 3 \times 6 \text{ mm}^3$	405.78	33.308	8.21%	498.90	72.586	14.55%	179.52	30.762	17.13%

### 3.3. Spectroscopy Measurements of a PMT with Different Scintillation Crystals and Different Gamma Sources Same as SiPM

In this part of study, the gamma ray spectrum acquired with Photo Multiplier Tube coupled to the scintillation crystals characterises the PMT features.

Figure 8 shows a high energy gamma source— $^{137}\text{Cs}$  spectrum acquired with Hamamatsu PMT coupled to different scintillation crystals of different size and density including CsI ( $4.51 \text{ g/cm}^3$  density:  $3 \times 3 \times 6 \text{ mm}^3$ ), LYSO ( $7.4 \text{ g/cm}^3$  density:  $2 \times 2 \times 5 \text{ mm}^3$ ) and GAGG (high density:  $3 \times 3 \times 6 \text{ mm}^3$ ) and NaI ( $3.67 \text{ g/cm}^3$  density: big size) From this figure and Table 2, it is concluded that NaI scintillation crystal with the biggest size—in comparison to other crystal—provides the better (lower) energy resolution. This is because of the bulky size of PMT vacuum tube requiring bigger size scintillation crystal to collect light photon. For instance, the energy resolution of  $^{137}\text{Cs}$  spectrum using PMT coupled to NaI was obtained 5.47% of FWHM which is comparable to 15.84%, 14.55% and 8.28% from CsI, GAGG and LYSO respectively.

The other comparison that can determine some information of the functionality of conventional PMT arises from Figure 9. These curves compare three different gamma ray spectrum obtained from the PMT coupled to the LYSO scintillation crystal. From this figure it can be concluded that the gamma sources of higher energy have lower energy resolution, therefore it can be preferred to use higher energy gamma sources instead of lower energy ones. In this research, the high-energy  $^{137}\text{Cs}$  spectrum using LYSO crystal coupled to PMT indicates a lower energy resolution of 8.28% of FWHM (good energy resolution), in comparison with  $^{22}\text{Na}$  (medium energy) and  $^{57}\text{Co}$  (low energy) with the energy resolution of 8.77% and 25.82%, respectively.

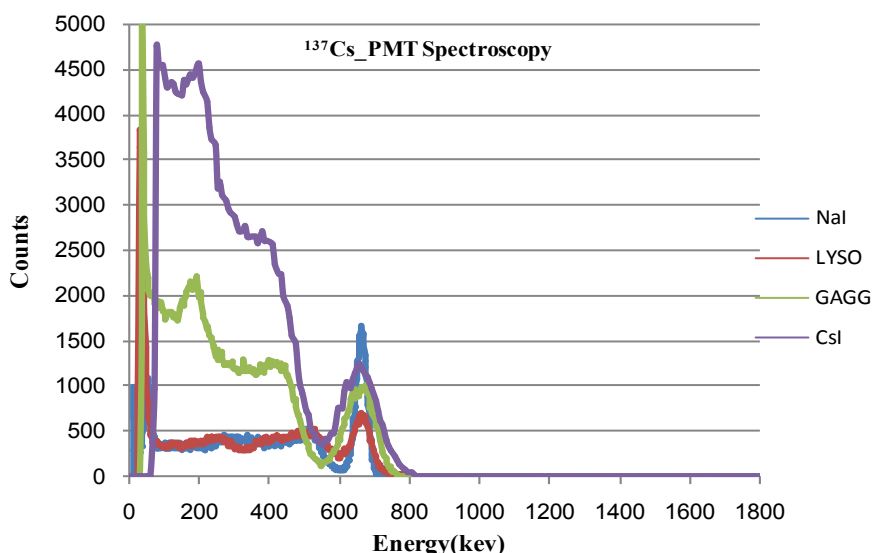


Figure 8. <sup>137</sup>Cs spectrum acquired with PMT coupled to NaI, LYSO, GAGG and CsI crystal.

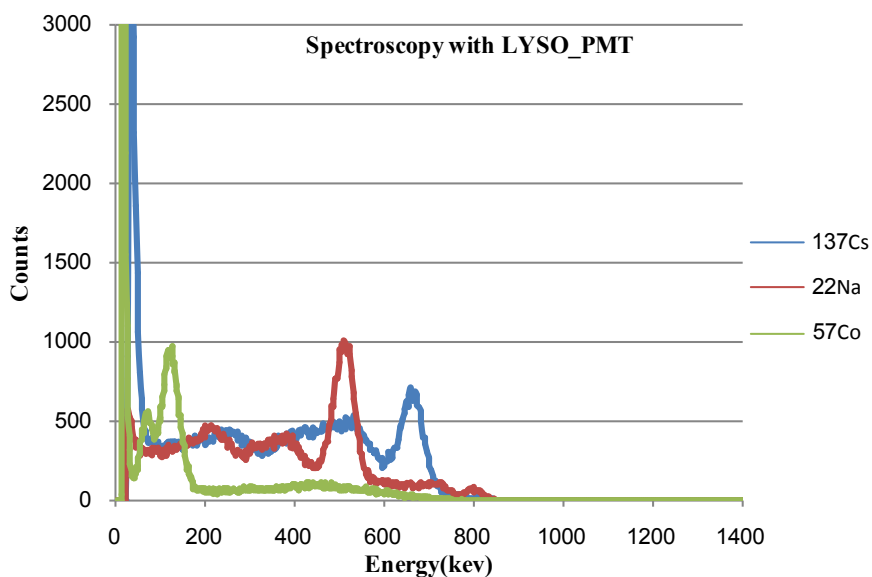


Figure 9. <sup>22</sup>Na, <sup>57</sup>Co and <sup>137</sup>Cs spectrum acquired with PMT coupled to LYSO crystal.

Table 2. Data taken from gamma ray spectrum of different gamma sources coupled to different scintillation crystals using PMT.

PMT	<sup>137</sup> CS (662 keV)			<sup>22</sup> Na (511 keV)			<sup>22</sup> CO (122 keV)		
	Centroid	FWHM	Energy resolution %FWHM	Centroid	FWHM	Energy resolution %FWHM	Centroid	FWHM	Energy resolution %FWHM
<b>CSI</b> 3 × 3 × 6 mm <sup>3</sup>	83.90	13.287	15.84%	51.41	8.163	15.87%	15.08	8.109	53.77%
<b>LYSO</b> 2 × 2 × 5 mm <sup>3</sup>	219.67	18.192	8.28%	197.94	17.359	8.77%	80.24	20.721	25.82%
<b>GAGG</b> 3 × 3 × 6 mm <sup>3</sup>	176.01	25.615	14.55%	135.23	20.918	15.47%	25.89	11.832	45.70%
<b>NaI</b>	468.97	25.680	5.47%	395.85	29.509	7.45%	270.11	44.480	16.47%

### 3.4. Comparative Spectroscopy Measurements of the SiPM and PMT

In this section, the spectrums acquired with photomultiplier tube and Silicon photomultiplier are compared. The energy resolutions obtained from these spectrums are compared in **Tables 3-5**. In addition, gamma ray spectrum with SiPM and PMT is compared (**Figure 10**). Based on the results from the comparison of PMT and SiPM, we can see that generally, the SiPM has better energy resolution than PMT. **Tables 3-5** show the differences of energy resolution between using SiPM and PMT with different scintillation crystal and gamma sources. For example, as it is seen from **Figure 3** and **Table 3**,  $^{137}\text{Cs}$  spectrum using GAGG crystal coupled to SiPM gives the energy resolution of 8.21% of FWHM. In contrast, using PMT in the same situation gives a comparable energy resolution of 14.55%. Therefore, the energy resolution of SiPM is lower and better than from PMT.

## 4. Conclusion

In this thesis, we have investigated a newly available SiPM array (ArraySM-4p9) from the SensL Inc. The performances of the SiPM array module were characterized in terms of their electrical and spectral properties. The electrical property of the SiPMs was investigated through direct measurement of its current-voltage (I-V) curve. The spectral property was investigated through the measurement of the gamma spectroscopy with different scintillation crystals as compared with a conventional PMT. The measured I-V curves show that each unit with  $4 \times 4$  SiPM pixels has very good performance uniformity. The channel-to-channel variations in breakdown voltage and dark currents are very consistent and stable. All the 16 SiPM pixels have the same breakdown voltage at 27.5 V. These indicate that this SiPM array device is of very good quality for applications. Our study also shows that this SiPM is well suitable for the common used scintillation crystals such as CsI(Tl) and LYSO as well as the newly available scintillator GAGG: Ce for broad energy-range gamma-ray detections. Gamma spectroscopy using  $^{57}\text{Co}$ ,  $^{22}\text{Na}$  and  $^{137}\text{Cs}$  sources shows that this SiPM device has well comparable spectral performance as the conventional PMT. The SiPM with CsI (Tl) and GAGG: Ce crystals using  $^{57}\text{Co}$  source show significantly better energy

**Table 3.** Data taken from  $^{137}\text{Cs}$  spectrum acquired with SiPM and PMT coupled to different scintillation crystals.

$^{137}\text{Cs}$ (662 keV)	SiPM			PMT		
	Centroid	FWHM	Energy resolution %FWHM	Centroid	FWHM	Energy resolution %FWHM
CSI ( $3 \times 3 \times 6 \text{ mm}^3$ )	238.89	27.709	11.60%	83.90	13.287	15.84%
LYSO ( $2 \times 2 \times 5 \text{ mm}^3$ )	229.56	21.228	9.25%	213.46	17.196	8.05%
GAGG ( $3 \times 3 \times 6 \text{ mm}^3$ )	405.78	33.308	8.21%	176.01	0.1455	14.55%

**Table 4.** Data taken from  $^{22}\text{Na}$  spectrum acquired with SiPM and PMT coupled to different scintillation crystals.

$^{22}\text{Na}$ (511 keV)	SiPM			PMT		
	Centroid	FWHM	Energy resolution %FWHM	Centroid	FWHM	Energy resolution %FWHM
CSI ( $3 \times 3 \times 6 \text{ mm}^3$ )	84.73	12.242	14.45%	51.41	8.163	15.87%
LYSO ( $2 \times 2 \times 5 \text{ mm}^3$ )	251.31	31.935	12.71%	197.94	17.359	8.77%
GAGG ( $3 \times 3 \times 6 \text{ mm}^3$ )	498.90	72.586	14.55%	135.23	20.918	15.47%

**Table 5.** Data taken from  $^{57}\text{Co}$  spectrum acquired with SiPM and PMT coupled to different scintillation crystals.

$^{57}\text{Co}$ (122 keV)	SiPM			PMT		
	Centroid	FWHM	Energy resolution %FWHM	Centroid	FWHM	Energy resolution %FWHM
CSI ( $3 \times 3 \times 6 \text{ mm}^3$ )	77.29	17.044	22.05%	15.08	8.109	53.77%
LYSO ( $2 \times 2 \times 5 \text{ mm}^3$ )	95.00	20.766	21.86%	80.24	20.721	25.82%
GAGG ( $3 \times 3 \times 6 \text{ mm}^3$ )	179.52	30.762	17.13%	112.96	48.025	42.51%

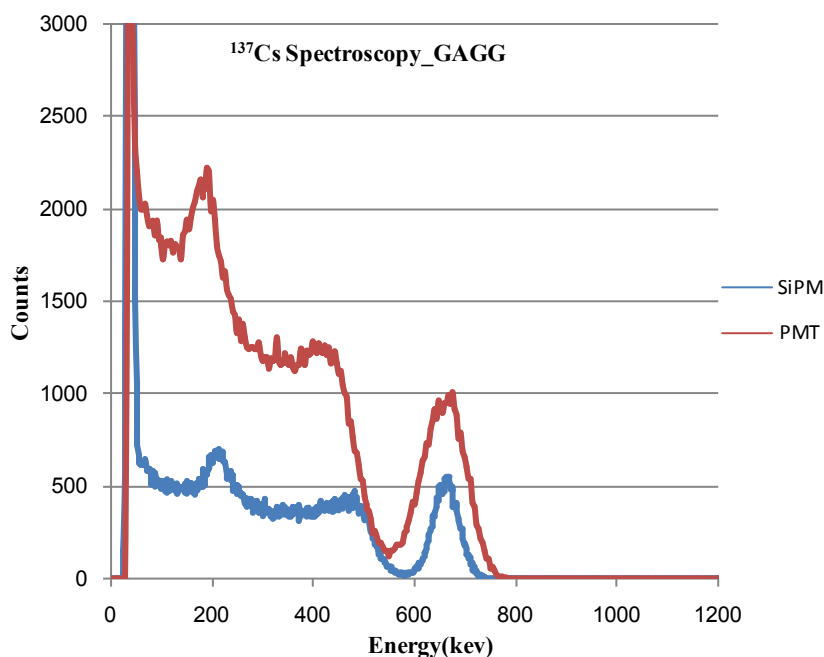


Figure 10.  $^{137}\text{Cs}$  spectrum acquired with PMT and SiPM coupled to GAGG crystal.

resolutions than the conventional PMT for the low energy gamma-ray detections. In conclusion, the newly available SiPMs have very good properties and are well suited with the most common used scintillation crystals for gamma-ray detections in a broad energy range. The SiPM has a great potential to replace the conventional PMT. Further study of this SiPM device for imaging application is under investigations.

## References

- [1] Ascenzo, N.D. and Saveliev, V. (2011) The New Photo-Detectors for High Energy Physics and Nuclear Medicine. In: Shi, J.-W., Ed., *Photodiodes—Communications, Bio-Sensings, Measurements and High-Energy Physics*, ISBN: 978-953-307-277-7, InTech.
- [2] Krizan, P. (2001) *IEEE Transactions on Nuclear Science*, **48**, 941-949. <http://dx.doi.org/10.1109/23.958704>
- [3] Bachri, A., Grant, P.C. and Goldschmidt, A. (2011) *Journal of the Arkansas Academy of Science*, **64**, 27-32.
- [4] Tafur, J., Van Wijk, E.P.A., Van Wijk, R. and Mills, P.J. (2010) *Photomedicine and Laser Surgery*, **28**, 23-30. <http://dx.doi.org/10.1089/pho.2008.2373>
- [5] Eckert, P., Schultz-Coulon, H.C., Shen, W., Stamen, R. and Tadday, A. (2010) *Nuclear Instruments and Methods in Physics Research A*, **620**, 217-226. <http://dx.doi.org/10.1016/j.nima.2010.03.169>
- [6] Garutti, E. (2011) *Journal of Instrumentation*, **6**, C10003. <http://dx.doi.org/10.1088/1748-0221/6/10/C10003>
- [7] Roncali, E. and Cherry, S.R. (2011) *Annals of Biomedical Engineering*, **39**, 1358-1377. <http://dx.doi.org/10.1007/s10439-011-0266-9>
- [8] Lee, J.S. and Hong, S.J. (2010) Geiger-Mode Avalanche Photodiodes for PET/MRI, *Electronic Circuits for Radiation Detection*. CRC Press, Boca Raton, 179.
- [9] Adamo, G., Parisi, A., Stivala, S., Tomasino, A., Agro, D., Curcio, L., Giaconia, G.C., Busacca, A. and Fallica, G. (2014) *IEEE Journal of Selected Topics in Quantum Electronics*, **20**, 1-7. <http://dx.doi.org/10.1109/JSTQE.2014.2346489>
- [10] Yoon, H.S., et al. (2012) *Journal of Nuclear Medicine*, **53**, 608-614. <http://dx.doi.org/10.2967/jnumed.111.097501>
- [11] Ko, G.B., et al. (2013) *Nuclear Instruments and Methods in Physics Research Section A*, **703**, 38-44. <http://dx.doi.org/10.1016/j.nima.2012.11.087>
- [12] Feng, S., Guang, L.J., Hong, L., Yu, W.H., Qian, M.Y., Tao, H., Li, Z., Xiao, C., Jun, S.L., Xiang, Y.B., Jian, F., Guang, X.Y., Hua, A.Z., Gang, W.Z., Min, G., Qiao, L.X., Bing, X.Y., Ping, W., Lei, S., Wu, Z., Zhen, X., Bang, L.H., Dong, W.X., Yun, Z.X., Heng, Z.Y., Cheng, M.X. and Hui, W. (2011) *Chinese Physics C (HEP & NP)*, **35**, 50-55.